ACES Asian Chemical Editorial Society

DOI: 10.1002/ajoc.201800552

ASIAN JOURNAL OF ORGANIC CHEMISTRY Communication

Drug Delivery

Photocleavable Supramolecular Polysaccharide Nanoparticles for Targeted Drug Release in Cancer Cells

Jiang-Hua Liu,[a] Xianjing Wu,[a] Ying-Ming Zhang,[a] and Yu Liu*[a, b]

Abstract: Photocontrolled, targeted and biocompatible supramolecular nanoparticles were constructed through the host-guest interactions of 2-nitrobenzyl ester-linked β-cyclodextrin and adamantane-grafted hyaluronic acid (HA). In this system, we used HA and 2-nitrobenzyl ester as targeting and photoresponsive groups, respectively. Moreover, the introduction of β-cyclodextrin further enhanced the biocompatibility of the supramolecular nanoparticles. Benefiting from the light-responsive capability of a 2-nitrobenzyl ester moiety, the hydrophobic anticancer drug camptothecin was loaded in the internal hydrophobic microenvironment of the supramolecular nanoparticle and could be specifically released in the cancer cells. These results demonstrated that supramolecular polysaccharide drug nanocarriers with targeting ability and intelligent light-stimulus responsiveness may have excellent potential in the clinical cancer treatments.

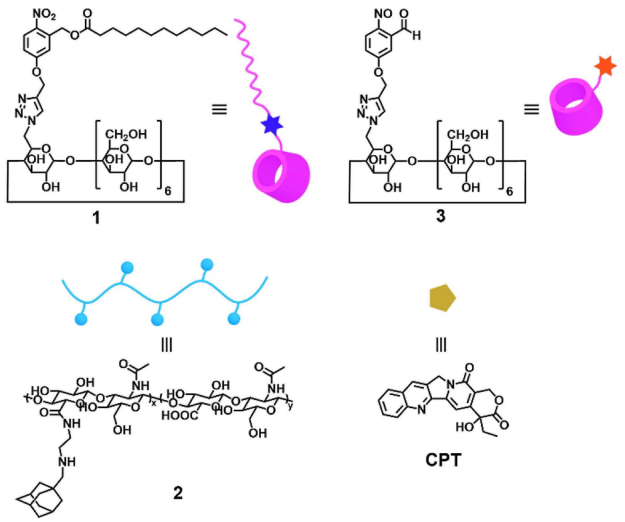

Figure 1. Molecular structures of host compound **1**, guest polymer **2**, reference compound **3**, and the anticancer drug **CPT**.

[a] *J.-H. Liu, X. Wu, Dr. Y.-M. Zhang, Prof. Y. Liu*
College of Chemistry, State Key Laboratory of Elemento-Organic Chemistry, Nankai University, Tianjin 300071, China
E-mail: yuliu@nankai.edu.cn

[b] *Prof. Y. Liu*
Collaborative Innovation Center of Chemical Science and Engineering (Tianjin), Tianjin 300072, China

Supporting information for this article is available on the WWW under https://doi.org/10.1002/ajoc.201800552

The application of nanocarriers for anticancer drug delivery has stimulated an upsurge of interest in the chemical and biomedical fields.[1] More intelligent drug nanocarriers with stimulus responsiveness and targeting ability have been delicately designed and constructed in the past decades, with the aim of promoting their practical translation in clinical use.[2] In this regard, the multistimuli-responsive supramolecular nanocarriers based on host-guest interactions provide a versatile nanoplatform in the construction of smart drug delivery systems and possess immense advantages, such as ease of synthesis, good reproducibility, favorable biocompatibility, and easier operability.[3] With the assistance of these supramolecular nanocarriers, many water-insoluble therapeutic drugs can be readily encapsulated in the hydrophobic cavities or microenvironments to enhance their water solubility and bioavailability and more significantly, the stimuli-sensitive sites and targeting agents can be conveniently introduced into the supramolecular nanocarriers by either covalent binding or noncovalent decoration.[4] Consequently, the multistimuli-responsive supramolecular nanocarriers, especially the ones based on functionalized macrocyclic receptors,[5] have shown great power in the battle against many degenerative diseases, such as cancers.

With these in mind, herein, we report a photo-responsive supramolecular nanoparticulate assembly,[6] which is constructed by the strong inclusion complexation between 2-nitrobenzyl ester-linked β-cyclodextrin (**1**) and adamantane-grafted hyaluronic acid (HA) (**2**). In our case, the HA skeleton possesses targeting ability to specifically recognize the overexpressed HA receptors on the cancer cells[7] and the 2-nitrobenzyl ester group can be photo-cleaved into 2-nitrosobenzaldehyde and carboxylic acid under UV light irradiation.[8] Meanwhile, the photocleavage of alkyl chain from the host compound can greatly alter the hydrophobic-hydrophilic balance of the whole supramolecular nanocarrier, eventually leading to the targeting transportation of water-insoluble anticancer drug camptothecin (CPT) in the cancer cells (Figure 1). Thus, it can be anticipated that our obtained binary assembly **1**⊂**2** with the targeted delivery and light-triggered drug release behaviors will open bright prospects in the cancer diagnostics and therapeutics.

First, we synthesized two host compounds **1** and **4** via "click chemistry" between compounds **6, 8** and mono-(6-deoxyl-6-azido)-β-CD, compounds **1** with 2-nitrobenzyl ester group as experimental host and the compound **4** without 2-nitrobenzyl group as reference host. The new compounds were compre-

hensively characterized by NMR and mass spectroscopy. On the other hand, the adamantane-grafted HA (**2**) as the polysaccharide shell was synthesized according to our previous work and the degree of substitution on **2** was calculated as one adamantane unit grafted on every five HA repeating sugar units on average according to the ^{1}H NMR spectra of **2**. The synthetic route and characterization of related compounds are shown in Scheme S1–S2 and Figure S1–S13. Next, the supramolecular assembly **1**⊂**2** could be conveniently constructed by simply mixing of **1** and **2** in aqueous solution, due to the moderate binding affinity between β-cyclodextrin (β-CD) and adamantane (ADA) moiety ($K_a > 4.0\times10^4$ M^{-1}).[9] Then, the binding modes between **1** and **2** were further investigated by ^{1}H NMR spectroscopy. As shown in Figure S14, the protons of ADA (H_{a-c}) exhibited a large downfield shift in the presence of **1**, which was definitely contributed to the tight intermolecular binding of ADA moiety with the cavity of β-CD.[10]

First, the photolysis performance of host **1** and assembly **1**⊂**2** were investigated by MALDI-TOF mass spectroscopy and UV-vis absorption spectra, respectively. As can be seen from Figure S6, before 365 nm UV light irradiation, the highest *m/z* peak in mass spectrum was located at 1571.5, corresponding to the molecular ion peak of host **1**. In contrast, after 365 nm UV light for 30 min, the *m/z* peak signal was changed to 1371.4, which could be clearly assigned to the photolysis product of **3** (Figure S15). This result clearly indicated that the *o*-nitrobenzyl group in **1** was converted to the 2-nitrosobenzaldehyde derivative. Meanwhile, UV-vis spectral changes further confirmed that the host **1** in the assembly **1**⊂**2** still possessed such photolysis property in the conversion from **1** to **3**. That is, a new absorption appeared at 350–400 nm and the spectral intensity accordingly increased upon exposure to 365 nm light irradiation, further indicative of the complete photolysis of the assembly **1**⊂**2** (Figure S16). Next, the CPT-loaded **1**⊂**2** nanoparticles (NPs) were prepared by slowly dropping CPT in MeOH ([CPT] = 5 μg/μL, 100 μL) into the aqueous solution of **1**⊂**2** assembly. The mixture solution was stirred for 24 hours in darkness and filtered with a 450 nm filter membrane to remove insoluble substance. The solution was dialyzed for 24 hours to obtain the solution of CPT-loaded **1**⊂**2** nanoparticles. Then the drug loading capability of **1**⊂**2** nanoparticles assembly was further investigated by UV-vis spectroscopy. According to the photometric standard curve of CPT, the drug loading efficiency and encapsulation efficiency of CPT were calculated on a weight/weight ratio as 2.8% and 11.7%, respectively, thereby corroborating that the anticancer drug CPT was efficiently loaded onto the **1**⊂**2** nanoparticles (Figure S17 and S18). It is also believed that the introduction of CPT could not interfere with the inclusion complexation in **1**⊂**2** assembly, because the binding stability between β-CD and CPT was fairly low (*ca.* 2.6×10^2 M^{-1}).[11]

Furthermore, dynamic light scattering (DLS) and transmission electron microscopic (TEM) experiments were performed to study the effect of UV light irradiation on the morphology and assembling size of CPT-loaded **1**⊂**2** nanoparticles. The DLS data showed that the hydrodynamic diameter of the binary nanoparticles was 151 nm before UV light irradiation and this value decreased to 128 nm after irradiation for 20 min, suggesting that the photocleavage of 2-nitrobenzyl ester group could lead to the formation of small-sized nanoassembly with more compact structure (Figure 2a). Moreover,

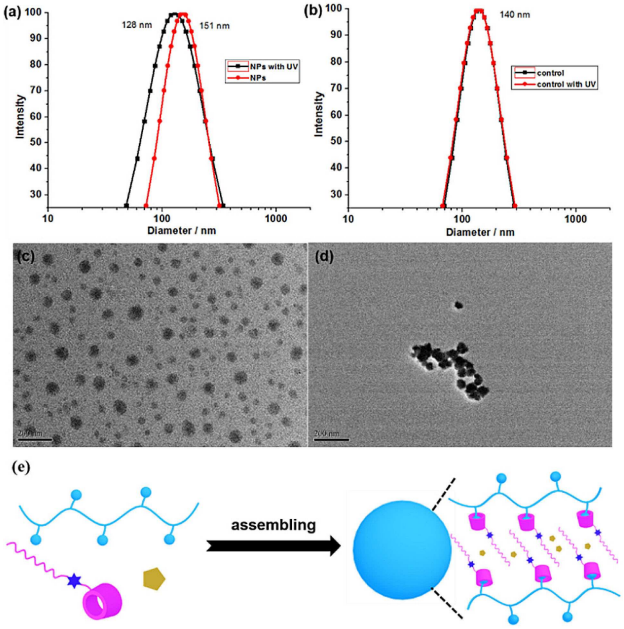

Figure 2. DLS data of (a) CPT-loaded **1**⊂**2** nanoparticles; (b) CPT-loaded **4**⊂**2** nanoparticles; TEM images of CPT-loaded **1**⊂**2** nanoparticles (c) before and (d) after 365 nm light irradiation; (e) the assembling process of CPT-loaded **1**⊂**2** nanoparticles.

some control experiments were carried out to further demonstrate the photolysis behaviors in the **1**⊂**2** nanoparticles. That is, no obvious change in the hydrodynamic diameter was observed after UV light irradiation using the CPT-loaded **4**⊂**2** and the reference host **4** without nitro group. This result clearly implied that the size changes of CPT-loaded **1**⊂**2** nanoparticles before and after UV light irradiation are exclusively contributed to the photolysis of 2-nitrobenzyl ester group (Figure 2b). Moreover, the TEM images also showed that the CPT-loaded **1**⊂**2** assembly dispersed as the spherical nanoparticles and more compact aggregates were found after UV light irradiation (Figure 2c and 2d). These results are consistent with the ones in DLS experiments.

The release of CPT was analyzed by monitoring the fluorescence intensity changes of CPT-loaded **1**⊂**2** nanoparticles under the UV light irradiation. As shown in Figure 3a, the fluorescence intensity of CPT-loaded **1**⊂**2** nanoparticles gradually decreased as the UV irradiation time increased to 18 min, indicating that the hydrophobic drug was gradually released into the aqueous phase because of the photocleavage of **1**. In sharp contrast, the fluorescence intensity of CPT-loaded **4**⊂**2** had no obvious change under the same experimental condition, indicating that CPT was tightly sealed in the hydrophobic region of the nanoparticles, because the host compound **4** without 2-nitrobenzyl group cannot be photo-decomposed (Figure S19). Accordingly, it could be calculated that about 60%

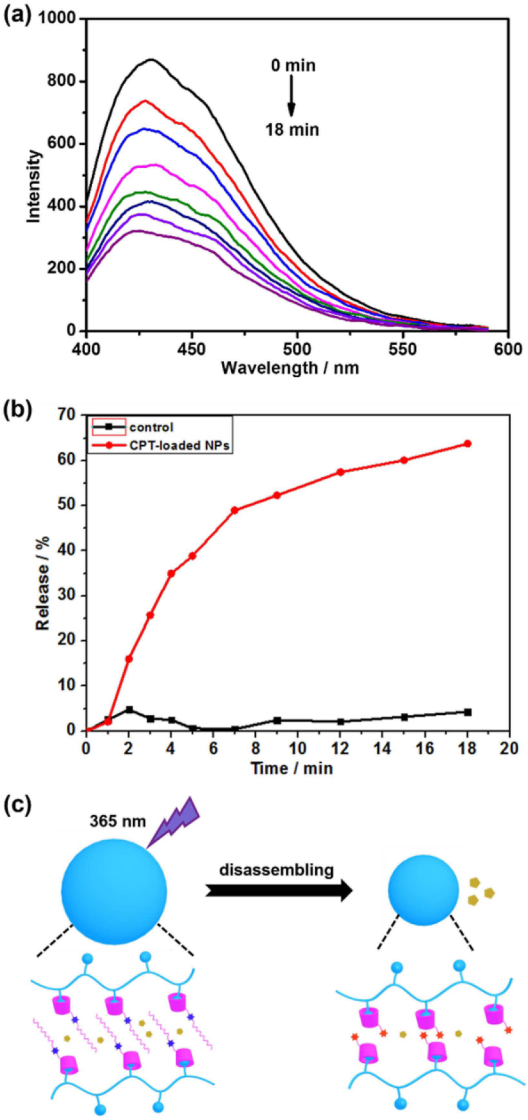

Figure 3. Fluorescence spectral changes of (a) CPT-loaded **1⊂2** nanoparticles under the UV light irradiation for 18 min; (b) drug release percentage of CPT-loaded **1⊂2** nanoparticles under the UV light irradiation for 18 min; (c) disassembling process of CPT-loaded **1⊂2** nanoparticles under UV irradiation.

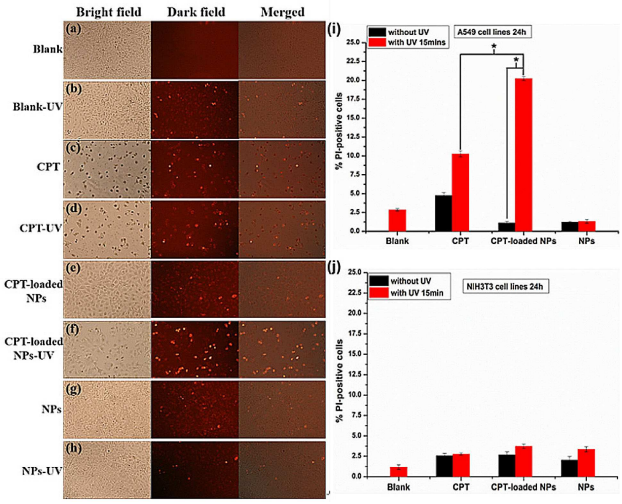

Figure 4. Bright field (left), dark field (middle) and merged (right) images of A549 cells after the treatment with (a) blank; (b) blank after UV irradiation at 365 nm for 15 min; (c) CPT; (d) CPT after UV irradiation at 365 nm for 15 min; (e) CPT-loaded **1⊂2** nanoparticles; (f) CPT-loaded **1⊂2** nanoparticles after UV irradiation at 365 nm for 15 min; (g) **1⊂2** nanoparticles; (h) **1⊂2** nanoparticles after UV irradiation at 365 nm for 15 min, in 24 h incubation. Cell viability assays of (i) A549 and (j) NIH3T3 cell lines in 24 h incubation. The treated cells were stained with PI and observed by fluorescence microscopy. The percent of PI-positive cells was calculated by the number of PI-positive cells divided by that of the total cells ×100. The asterisk indicates significant difference in the examined groups ($^*p < 0.05$).

CPT was released from **1⊂2** nanoparticles after UV light irradiation in 18 min, whereas no CPT was released in the control experiment (Figure 3b and 3c).

Finally, cells viability assays were further performed to evaluate the targeted anticancer activity of CPT-loaded supramolecular nanoparticles *in vitro* by using the propidium iodide (PI)-staining method (Figure 4). No obvious change in cell viability was observed in the normal fibroblast NIH3T3 cells and A549 cancer cells before and after UV light irradiation for 15 min, indicating that the UV light irradiation in such a short time had a negligible effect on the cell viability. Moreover, after incubation for 24 h with or without UV light irradiation, the cell death rate of **1⊂2** nanoparticles both in NIH3T3 and A549 cell lines remained at a low rate (3.5%). The result revealed that the **1⊂2** nanoparticles possessed the very low cytotoxicity and good biocompatibility. In sharp contrast, it is noteworthy that the anticancer activity towards A549 cancer cells of CPT-loaded **1⊂2** nanoparticles under UV light irradiation for 15 min was ten times higher than that without UV light irradiation. These phenomena jointly demonstrated that the drug molecules were released from CPT-loaded **1⊂2** nanoparticles in a photo-controlled manner. In comparison, given that there was no abundant HA receptors over-expressed in the cell membranes, the cytotoxicity of CPT-loaded binary nanoparticles toward the normal NIH3T3 cells was fairly low before and after UV light irradiation, further indicating that our obtained nanoparticles could specifically recognize the cancer cells. In addition, after 24 h incubation, the CPT-loaded **1⊂2** nanoparticles gave 20.3% PI-positive cells towards A549 cancer cell line under UV light irradiation, which was much higher than the corresponding value of pristine CPT (10.3%). This result suggested that the supramolecular nanoparticles could enhance anticancer efficacy to a great extent, probably due to the improved bioavailability when CPT was entrapped in the hydrophobic microenvironment of nanocarriers. Meanwhile, the PI staining images showed that compared to the A549 cell line, the experimental groups in NIH3T3 cells had a very low percentage in cell death when treated with the **1⊂2** nanoparticles under UV light irradiation (Figure 4i and 4j). It is also found that there was a dose-dependent cell viability under our experimental condition; that is, the CPT-loaded **1⊂2** nanoparticle could kill nearly 100% cancer cells at the CPT concentration of 16.8 μg/mL after UV irradiation for 15 min. In sharp contrast, the corresponding cell death rates were fairly low for normal cells under the same experimental condition (Figure S20). Meanwhile, the cell mor-

phological characteristics of cancer and normal cells were consistent with results obtained from the cells viability assays (Figures 4a–4h and S21). Taken together, all the aforementioned results revealed that the anticancer drug CPT could be endowed with photo-sensitivity delivery and targeted ability after encapsulation in the **1**⊂**2** nanoparticles.

In conclusion, by taking advantage of the strong host-guest complexation of β-CD and adamantyl group, we have successfully constructed photo-controlled, targeted and biocompatible supramolecular nanoparticles by the supramolecular complexation between **1** and **2**, which could efficiently load anticancer drug CPT into the hydrophobic region of nanocarrier. Under the 365 nm light irradiation for only 18 min, the hydrophobic drug CPT was gradually released into the aqueous environment from **1**⊂**2** nanoparticles, because the photocleavage of **1** could disrupt the hydrophilic-hydrophobic balance of the supramolecular nanoparticles. Moreover, the *in vitro* cytotoxicity experiments further indicated that the CPT-loaded **1**⊂**2** nanoparticles exhibited better anticancer activity than free CPT toward A549 cancer cells, but the cytotoxicity was fairly low to the normal cells. Thus, we can envision that the **1**⊂**2** nanoparticles with remotely controlled and specially targeted drug release and delivery behaviors may have great potential in the cancer therapy.

Acknowledgements

This work was financially supported by the National Natural Science Foundation of China (grants 21432004, 21472100, 21772099, and 91527301).

Conflict of Interest

The authors declare no conflict of interest.

Keywords: polysaccharide nanocarriers · photocleavage · drug delivery · cyclodextrins · hyaluronic acid

[1] a) D. Rosenblum, N. Joshi, W. Tao, J. M. Karp, D. Peer, *Nat. Commun.* **2018**, *9*, 1410;b) S. Mura, J. Nicolas, P. Couvreur, *Nat. Mater.* **2013**, *12*, 991–1003; c) S.-Y. Qin, A.-Q. Zhang, S.-X. Cheng, L. Rong, X.-Z. Zhang, *Biomaterials* **2017**, *112*, 234–247; d) S.-Y. K. Bhattacharyya, S. Mukherjee, *Bull. Chem. Soc. Jpn.* **2018**, *91*, 447–454; e) J. Li, C. Sun, W. Tao, Z. Cao, H. Qian, X. Yang, J. Wang, *Biomaterials* **2018**, *170*, 147–155.

[2] a) M. Karimi, A. Ghasemi, P. S. Zangabad, R. Rahighi, S. M. M. Basri, H. Mirshekari, M. Amiri, Z. S. Pishabad, A. Aslani, M. Bozorgomid, M. R. Hamblin, *Chem. Soc. Rev.* **2016**, *45*, 1457–1501; b) X. Wu, Y.-M. Zhang, Y. Liu, *RSC Adv.* **2016**, *6*, 99729–99734; c) B.-L. Li, M. I. Setyawati, L. Chen, J. Xie, K. Ariga, C.-T. Lim, S. Garaj, D. T. Leong, *ACS Appl. Mater. Interfaces* **2017**, *9*, 15286–15296.

[3] a) M. Nakahata, Y. Takashima, H. Yamaguchi, A. Harada, *Nat. Commun.* **2011**, *2*, 511; b) Y.-M. Zhang, Y. Yang, Y.-H. Zhang, L. Yu, *Sci. Rep.* **2016**, *6*, 28848; c) M. Zan, J. Li, S. Luo, Z. Ge, *Chem. Commun.* **2014**, *50*, 7824–7827; d) Q. Zhao, Y. Chen, M. Sun, X.-J. Wu, Y. Liu, *RSC Adv.* **2016**, *6*, 50673–50679; e) Q. Yu, Y.-M. Zhang, Y.-H. Liu, X. Xu, Y. Liu, *Sci. Adv.* **2018**, *4*, eaat2297.

[4] a) K. M. Wiggins, J. N. Brantley, C. W. Bielawski, *ACS Macro Lett.* **2012**, *1*, 623–626; b) D. Yang, W. Chen, J. Hu, *J. Phys. Chem. B* **2014**, *118*, 12311–12317; c) B. E. Hirsch, K. P. Mcdonald, Q. Bo, A. H. Flood, S. L. Tait, *ACS Nano.* **2014**, *8*, 10858–10869.

[5] a) H. Zhao, E. S. Sterner, E. B. Coughlin, P. Theato, *Macromolecules* **2012**, *45*, 1723–1736; b) S. Iamsaard, S. J. ßhoff, B. Matt, T. Kudernac, J. J. Cornelissen, S. P. Fletcher, N. Katsonis, *Nat. Chem.* **2014**, *6*, 229; c) M. Rabnawaz, G. Liu, *Macromolecules* **2012**, *45*, 5586–5595; d) Z. C. Smith, D. M. Meyer, M. G. Simon, C. Staii, D. Shukla, S. W. Thomas, *Macromolecules* **2015**, *48*, 959–966; e) J. Erath, J. Cui, J. Schmid, M. Kappl, C. A. Del, A. Fery, *Langmuir* **2013**, *29*, 12138–12144.

[6] a) I. J. Majoros, T. P. Thomas, C. B. Mehta, J. R. Baker, *J. Med. Chem.* **2005**, *48*, 5892–5899; b) R. P. Feazell, N. N. Ratchford, H. Dai, S. J. Lippard, *J. Am. Chem. Soc.* **2007**, *129*, 8438–8439.

[7] a) K. Y. Choi, H. Chung, K. H. Min, H. Y. Yoon, K. Kim, J. H. Park, I. C. Kwon, S. Y. Jeong, *Biomaterials* **2010**, *31*, 106–114; b) Y. Yang, Y.-M. Zhang, Y. Chen, J.-T. Chen, Y. Liu, *J. Med. Chem.* **2013**, *56*, 9725–9736.

[8] a) P. Neveu, I. Aujard, C. Benbrahim, S. T. Le, J. F. Allemand, S. Vriz, D. Bensimon, L. Jullien, *Angew. Chem. Int. Ed.* **2010**, *47*, 3744–3746; b) G. Delaittre, T. Pauloehrl, M. Bastmeyer, C. Barnerkowollik, *Macromolecules* **2012**, *45*, 1792–1802; c) N. Fomina, J. Sankaranarayanan, A. Almutairi, *Adv. Drug Delivery Rev.* **2012**, *64*, 1005–1020; d) M. Goard, G. Aakalu, O. D. Fedoryak, C. Quinonez, J. S. Julien, S. J. Poteet, E. M. Schuman, T. M. Dore, *Chem. Bio.* **2005**, *12*, 685–693; e) C. G. Bochet, *J. Chem. Soc.* **2002**, *2*, 125–142.

[9] a) M. R. Eftink, M. L. Andy, K. Bystrom, H. D. Perlmutter, D. S. Kristol, *J. Am. Chem. Soc.* **1989**, *20*, 6765–6772; b) B. Yan, J. C. Boyer, N. R. Branda, Y. Zhao, *J. Am. Chem. Soc.* **2011**, *133*, 19714–19717.

[10] L.-X. Chen, Y.-M. Zhang, Y. Cao, H. Y. Zhang, Y. Liu, *RSC Adv.* **2016**, *6*, 28593–28598.

[11] J. Kang, V. Kumar, D. Yang, P. R. Chowdhury, R. J. Hohl, *Eur. J. Pharm. Sci.* **2002**, *15*, 163–170.

Manuscript received: September 18, 2018
Accepted manuscript online: October 15, 2018
Version of record online: October 31, 2018